Optimized solid-state synthesis of LiFePO$_4$ cathode materials using ball-milling

Hee-Cheol Kang [a], Dae-Kyoo Jun [a], Bo Jin [b,a], En Mei Jin [a],
Kyung-Hee Park [a], Hal-Bon Gu [a,*], Ki-Won Kim [c]

[a] Department of Electrical Engineering, Chonnam National University, Gwangju 500-757, South Korea
[b] College of Materials Science and Engineering, Jilin University, Changchun 130025, China
[c] ITRC for Energy Storage and Conversion, Gyeongsang National University, Jinju 660-701, South Korea

Abstract

Olivine-type LiFePO$_4$ cathode materials were synthesized by a solid-state reaction method and ball-milling. The ball-milling time, heating time and heating temperature are optimized. A heating temperature higher than 700 °C resulted in the appearance of impurity phase Fe$_2$P and growth of large particle, which was shown by high resolution X-ray diffraction and field emission scanning electron microscopy. The impurity phase Fe$_2$P exhibited a considerable capacity loss at the 1st cycle and a gradual increase in discharge capacity upon cycling. Moreover, it exhibited an excellent high-rate capacity of 104 mAh g^{-1} at 3 C in spite of the large particle size. The optimum synthesis conditions for LiFePO$_4$ were ball-milling for 24 h and heat-treatment at 600 °C for 3 h. LiFePO$_4$/Li cells showed an enhanced cycling performance and a high discharge capacity of 160 mAh g^{-1} at 0.1 C.
© 2008 Elsevier B.V. All rights reserved.

Keywords: LiFePO$_4$; Solid-state reaction; Ball-milling; Fe$_2$P

1. Introduction

There is an increasing demand for batteries with a high energy density for use in hybrid electric vehicles (HEVs), power storage, portable electronic devices, etc. [1–3]. LiCoO$_2$ is used as the cathode material for commercial lithium batteries [4], but its high cost, environmental pollution and thermal instability have created a demand for alternative materials. LiFePO$_4$ is a promising candidate due to its ability to provide long cycle life and high rate in spite of high temperatures [5–8]. LiFePO$_4$ has a two-phase reaction of LiFePO$_4$/FePO$_4$ and an excellent theoretical capacity of 170 mAh g^{-1} based on Fe^{2+}/Fe^{3+} leading to very flat voltage curve with a plateau around 3.4 V vs. Li/Li$^+$ [9,10]. Nevertheless, it is difficult to make practical use of the full theoretical capacity at high rate, because the separation of the chain of FeO$_6$ edge-shared octahedral contributes an

extremely low electronic conductivity [5–11]. Many researchers have suggested solutions to this problem as follows: (i) coating with a conductive layer around the particles [12]; (ii) ionic substitution to enhance the electrochemical properties [13–15] and (iii) synthesis of particles with well-defined morphology [16].

Olivine-type LiFePO$_4$ can be synthesized by a solid-state reaction method [5,6,8,9,11,14,17], by sol–gel [18], by mechanical activation (MA) [19–21], by microwave heating [22], etc. Among these methods, olivine-type LiFePO$_4$ has been heat-treated at >600 °C [8]. The solid-state reaction has been widely adopted for synthesis of pure crystalline olivine-phase LiFePO$_4$; however, this method is complex, including repeated grinding to gain homogenous particles and several steps at high temperature to impede formation of the impurity phase. This repeated heating treatment results in the formation of large particles [6,17].

In other synthetic methods, the effect of using ball-milling to synthesize LiFePO$_4$ has been reported by several research groups [19–21,23]. In recent studies, MA methods have been

investigated for the synthesis of LiFePO$_4$ in which the starting materials are mixed for production of the precursor in a high-energy, shaker-type ball-mill (>1000 rpm), followed by a one-step thermal treatment of the compound [20,21]. It has been reported that the impurity Fe$_2$P phase appears during heating treatment at high temperature (>700 °C); nevertheless, the time and cost of thermal treatment for well-crystallized LiFePO$_4$ can be decreased by this process.

In this study, LiFePO$_4$ was synthesized by a solid-state reaction method and ball-milling procedure in which a planetary mono-mill was used to mix the starting materials at a low speed (300 rpm), and LiFePO$_4$ was synthesized by a one-step thermal treatment. The synthesis conditions, such as heating time, heating temperature and ball-milling time were investigated by high-resolution X-ray diffraction (HR-XRD), field emission scanning electron microscopy (FE-SEM) and charge–discharge experiments to evaluate the electrochemical performance of LiFePO$_4$ as a cathode material.

2. Experimental

LiFePO$_4$ was prepared by the solid-state reaction of stoichiometric amounts of Li$_2$CO$_3$, FeC$_2$O$_4$·2H$_2$O and NH$_4$H$_2$PO$_4$ (all from Aldrich). The precursors were mixed by ball-milling (Planetary Mono-Mill, FRITCH) in N-methyl-2-pyrolidinone (NMP, Aldrich) at 300 rpm for various lengths of time and then dried at 90 °C for 24 h. Ball-milling was carried out at room temperature in air using a zirconia vial and balls (ball/powder weight ratio 5:2). The mixture was pelleted and heated in a nitrogen atmosphere at various temperatures from 550 °C to 700 °C for various lengths of time. All heating and cooling rates were 5 °C min^{-1}.

The mixed composite powders were analyzed by thermogravimetric analyzer. The crystalline phase of the synthesized powders was obtained using HR-XRD (D/MAX Uitima III, Rigaku) with Cu Kα radiation and the morphological properties were observed by FE-SEM (S-4700, Hitachi).
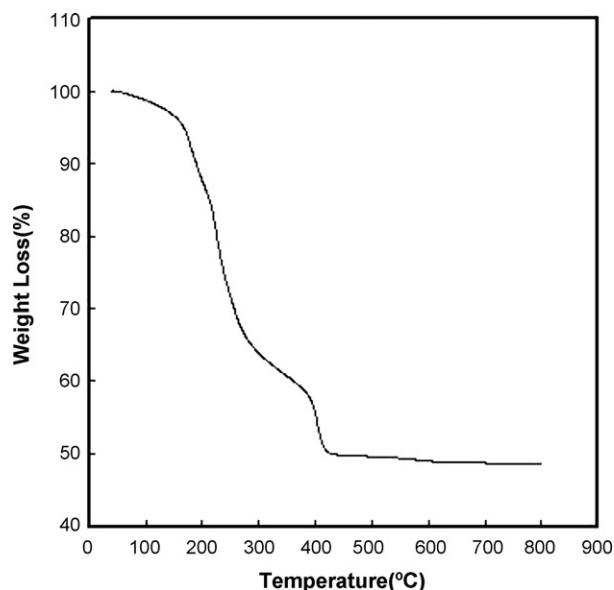
For the electrochemical testing, the composite electrodes were fabricated using as-prepared cathode materials, carbon black and polyvinylidene fluoride (PVDF) with a weight ratio of 70:20:10 in NMP. The slurry was coated onto Al foil and dried at 90 °C for 1 h before roll-pressing, and then the electrodes were dried again at 110 °C for 24 h under vacuum. The cells were assembled in argon-filled glove box using lithium as the anode and 1 M LiPF$_6$/EC-DEC (1:1 vol%) as the electrolyte. Cyclic voltammetry (CV) was performed at a scan-rate of 0.1 mV s^{-1} from 2.3 V to 4.5 V. The charge–discharge cycle performance was examined in galvanostatic charge–discharge unit WBCS-3000 battery cycler from 2.5 V to 4.0 V at a constant current density of 0.1 mA cm^{-2} at 25 °C.

Fig. 1. TG curve of LiFePO$_4$ at a heating rate of 10 °C min^{-1} in nitrogen.
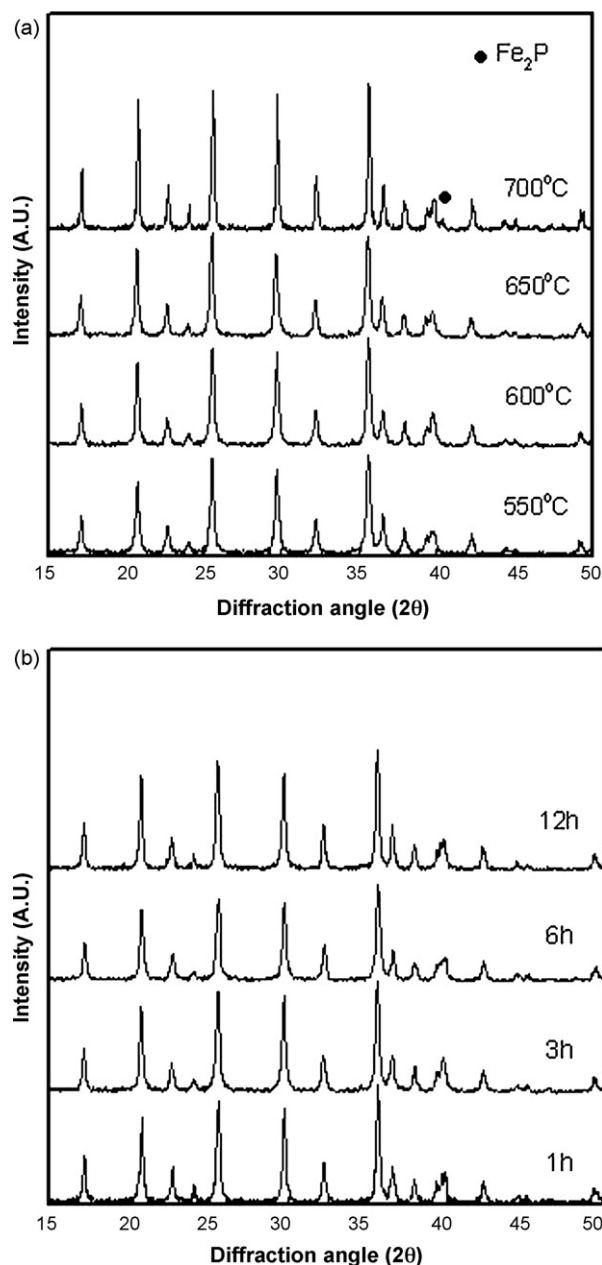

Fig. 2. XRD spectra of LiFePO$_4$ prepared (a) at various temperatures for 3 h and (b) at 600 °C for different lengths of time (ball-milling for 24 h).

3. Results and discussion

The thermogravimetry (TG) curve of mixed powders used to prepare LiFePO$_4$ is shown in Fig. 1. TG analysis is used to determine the appropriate temperature for the heat treatment. The TG curve exhibited 50% weight loss until 420 °C due to decomposition of FeC$_2$O$_4$·2H$_2$O and its reaction with the decomposed product of NH$_4$H$_2$PO$_4$, and then the product weight decreases slightly at temperatures >500 °C. From the above results for TG analysis, temperatures above 500 °C were chosen to prepare LiFePO$_4$.

To confirm the suitability of the heating conditions chosen, a simple one-step heating treatment at various temperatures for different lengths of time was carried out. The results of the XRD patterns of samples prepared under various heating conditions are shown in Fig. 2. All diffraction peaks of the samples were identified as belonging to the orthorhombic crystal structure. However, impurity phase Fe$_2$P around $2\theta = 40°$ was detected in the sample prepared at 700 °C for 3 h (Fig. 2(a)). Several researchers have suggested that Fe$_2$P has a high electronic conductivity of $\sim 10^{-2}$ S cm^{-1}, which is formed by a carbonthermal reaction at high temperature, with an increased electronic conductivity of LiFePO$_4$ and a decreased ionic conductivity of LiFePO$_4$ [20,24–26]. As shown by XRD, the generation of impurity phase Fe$_2$P can be realized by heating at 700 °C.

The effect of heating temperature was investigated by FE-SEM and the images are shown in Fig. 3. The samples prepared at 550 °C, 600 °C and 650 °C consist of non-uniform fine particles with a size range of 100–400 nm, as shown in Fig. 3(a)–(c). However, the particle size of LiFePO$_4$ prepared at 700 °C is considerably larger, as shown in Fig. 3(d). The growth of particle size was reflected as a low electrical conductivity and slow diffusion of the lithium ions during charge–discharge [16,27–29].

The samples heated at 600 °C and 700 °C were examined by cyclic voltammetry to compare pure LiFePO$_4$ with LiFePO$_4$ containing Fe$_2$P. The cells were tested between 2.3 V and 4.5 V at a scanning rate of 0.1 mV s^{-1}, and the results are shown in Fig. 4. This indicates that Fe^{2+}/Fe^{3+} redox-pairs contribute to the gain and loss of electrons in the crystal structures of both samples during the lithium insertion/extraction process. However, the cathodic and anodic peak intensities of LiFePO$_4$ containing Fe$_2$P prepared at 700 °C were much larger than that of pure LiFePO$_4$. The difference between the cathodic and anodic peaks decreased upon cycling, demonstrating that the reversible electrochemical reaction of LiFePO$_4$ is enhanced due to improvement of the electronic conductivity by Fe$_2$P.

The discharge curves for the 10th and 20th samples prepared from 550 °C to 700 °C are shown in Fig. 5. The discharge potential plateaus of samples were at 3.4 V vs. Li/Li$^+$, except for the sample prepared at 550 °C. However, discharge potential plateau of sample prepared at 700 °C is improved at the
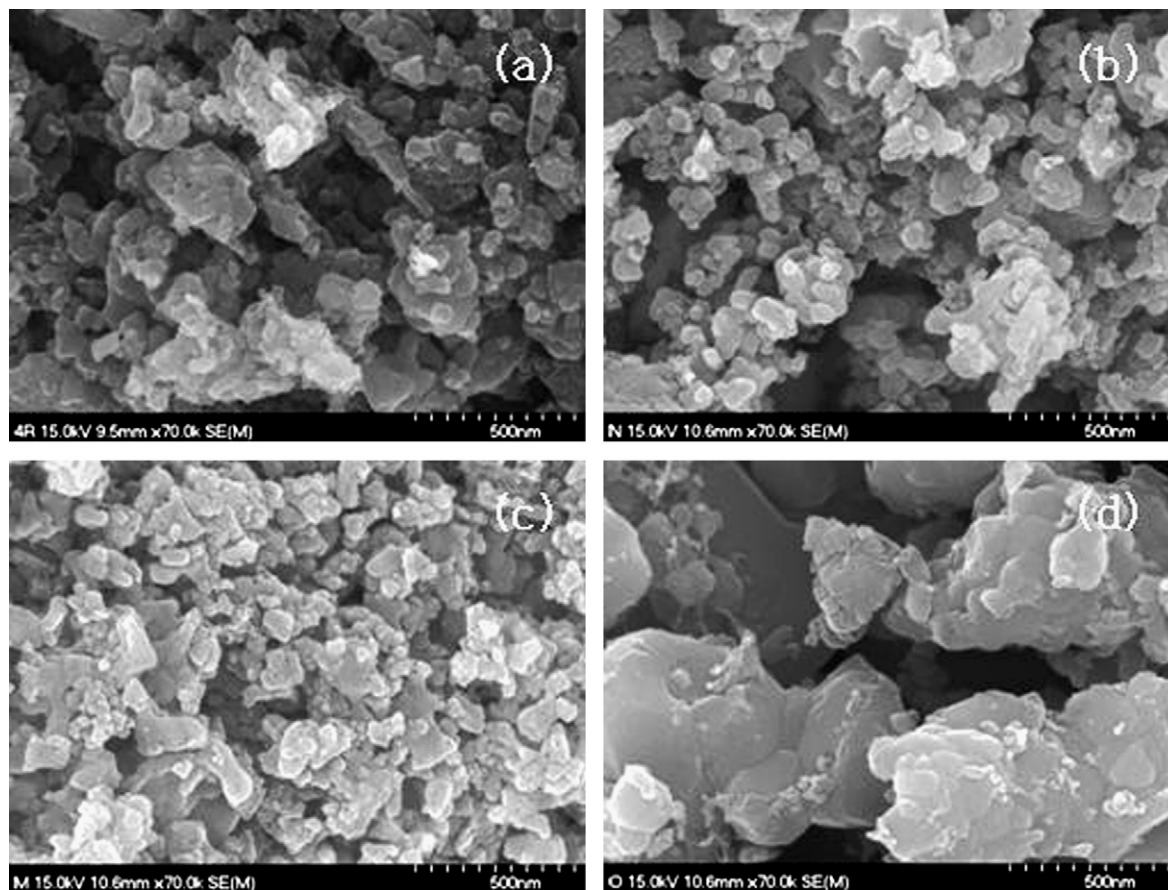

Fig. 3. FE-SEM images of LiFePO$_4$ prepared at (a) 550 °C, (b) 600 °C, (c) 650 °C and (d) 700 °C (thermal treatment for 3 h).
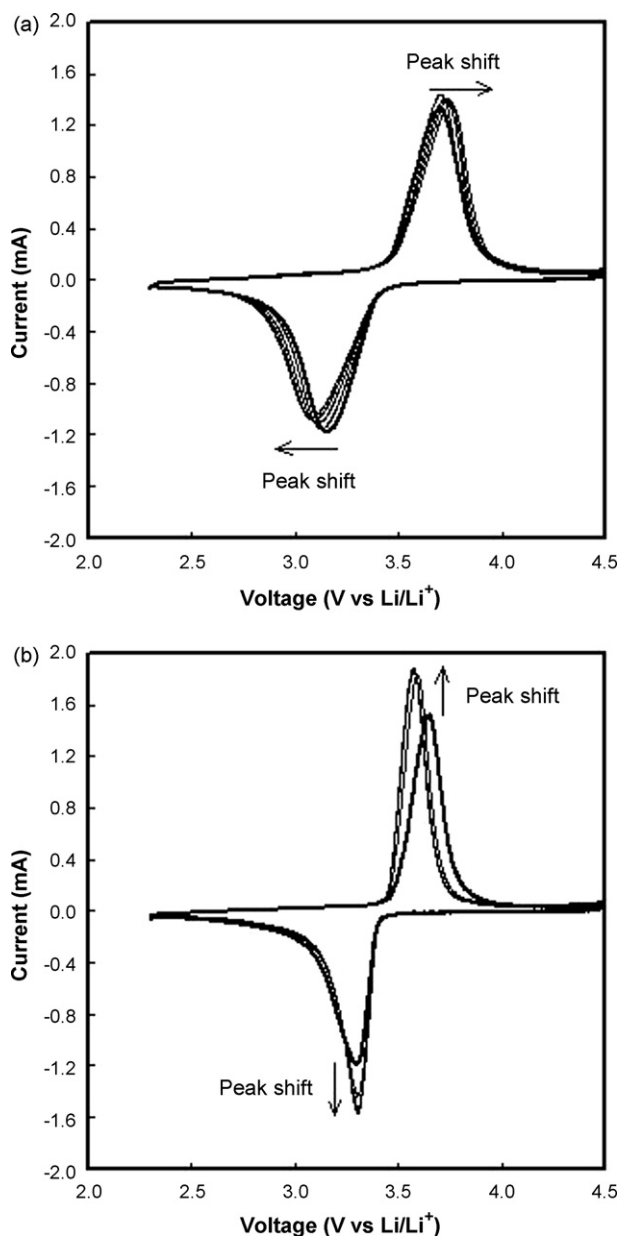
Fig. 4. Cyclic voltammograms of LiFePO$_4$ prepared at (a) 600 °C and (b) 700 °C.

Fig. 5. The discharge curves of LiFePO$_4$ prepared at (a) 550 °C, (b) 600 °C, (c) 650 °C and (d) 700 °C (at the 10th and 20th cycles). The inset shows the corresponding cycle ability of the samples.

20th cycle compared with the other samples. The cycling performance of these samples is shown in the inset of Fig. 5. The cell of samples heated at 600 °C can deliver a discharge capacity of 140 mAh g^{-1} at the 1st cycle. The discharge capacity of other samples was increased slightly in the initial few cycles and then stabilized upon cycling. The similar phenomenon has been reported elsewhere [19,30–32]. Zhang et al. [31] suggested that such phenomena were associated with self-doping of Li$^+$ ions into the Fe site during the initial cycles, which increased the electronic conductivity of the bulk of the LiFePO$_4$ cathode resulting in enhanced capacity. However, the sample prepared at 700 °C had a gradual increase of discharge capacity until the 50th cycles, as shown in the inset of Fig. 5. It is likely that the growth of large particles leading to little intercalation/deintercalation of lithium
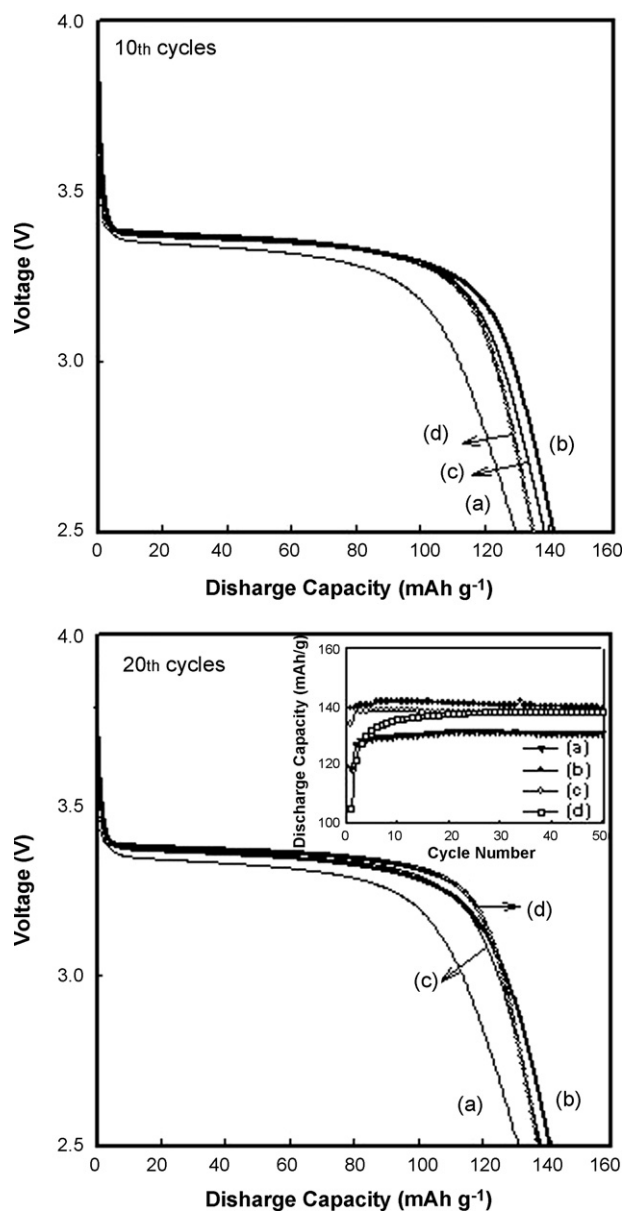
ions results in an initial loss of discharge capacity and a gradual increase of capacity upon cycling is due to an effect of Fe$_2$P, which has a high level of electronic conductivity [26].

The morphological properties of samples prepared at the optimum temperature of 600 °C for different lengths of time are described in Fig. 6. The sample prepared for 1 h consists of small clusters and agglomerates with an average particle size < 400 nm, and sample prepared for 3 h had a slightly smaller particle size, as shown in Fig. 6(b). In contrast, heating for 6 h and 12 h causes the small clusters to fuse together into large agglomerates, as shown in Fig. 6(c) and (d). It is clear that the average particle size increases with increasing heating time.

The discharge capacity of these samples upon cycling is shown in Fig. 7. As expected from the FE-SEM results, the sam-
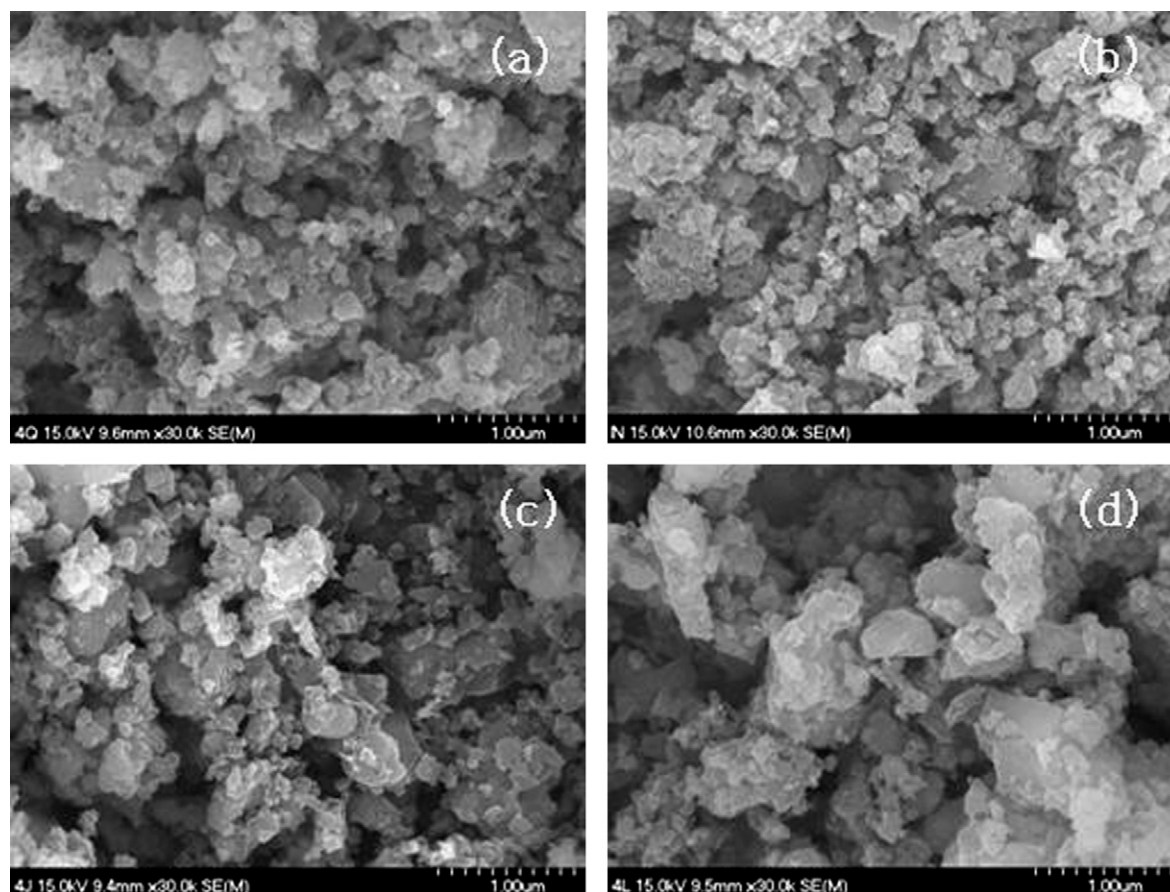
Fig. 6. FE-SEM images of LiFePO$_4$ prepared at 600 °C for (a) 1 h, (b) 3 h, (c) 6 h and (d) 12 h.

ple prepared for 3 h had the smallest particle size and a higher discharge capacity and a more stable cycle life than the others, as shown in Fig. 7(b). However, other samples had a similar trend of cyclic performance, with an initial loss of capacity and
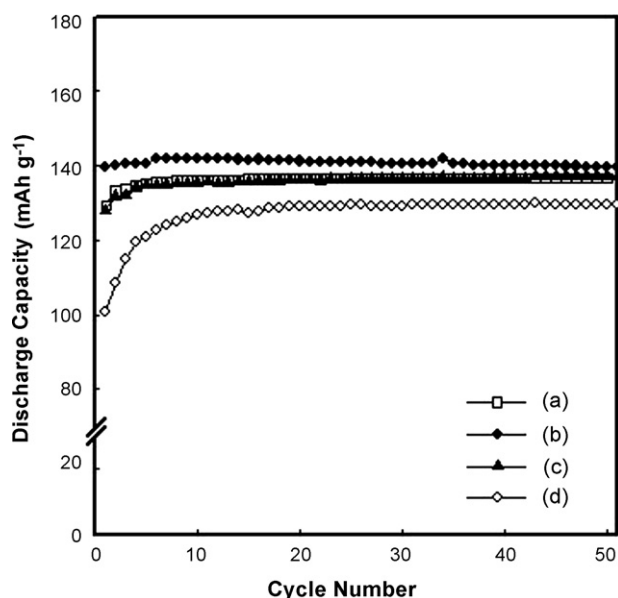

Fig. 7. The discharge capacity of LiFePO$_4$ prepared at 600 °C for (a) 1 h, (b) 3 h, (c) 6 h and (d) 12 h.

stability of the cycle performance after a few cycles, as shown in Fig. 7(a) and (c). It is especially clear for the sample prepared for 12 h, which consists of particles >500 nm and had the lowest discharge capacity in the initial cycle and a considerable increase in capacity until the 10th cycle. This is likely due to the growth of particle size leading to little intercalation/deintercalation of lithium ions for a few initial cycles, even though the impurity phase Fe$_2$P is not detected by XRD. On the basis of previous results, it is concluded the optimal thermal treatment condition to obtain pure LiFePO$_4$ using ball-milling is 600 °C for 3 h.

The morphological properties of powders mixed by ball-milling are shown in Fig. 8. These mixing precursors were heat-treated commonly at 600 °C for 3 h. The particle size was slightly smaller with increased ball-milling time. Moreover, the average crystallite size of the samples prepared for ball-milling times of 6 h, 12 h, 24 h and 36 h is estimated to 44.34 nm, 42.79 nm, 37.11 nm and 35.76 nm, respectively. The crystallite size of the samples was calculated using the Scherrer equation: $\sigma = 0.9\lambda/(\beta_{2\theta}\cos\theta)$, from the full-width-at-half-maximum β of four strong and well-resolved reflection peaks corresponding to the [1 0 1], [1 1 1], [2 1 1] and [3 1 1] crystallographical directions from XRD (data not shown). FE-SEM observations and the calculated crystallite size suggest that the small precursor contributes to formation of small crystallites. The initial small precursor is expected to react well during thermal treatment due to increased contact surface area between the precursor particles.
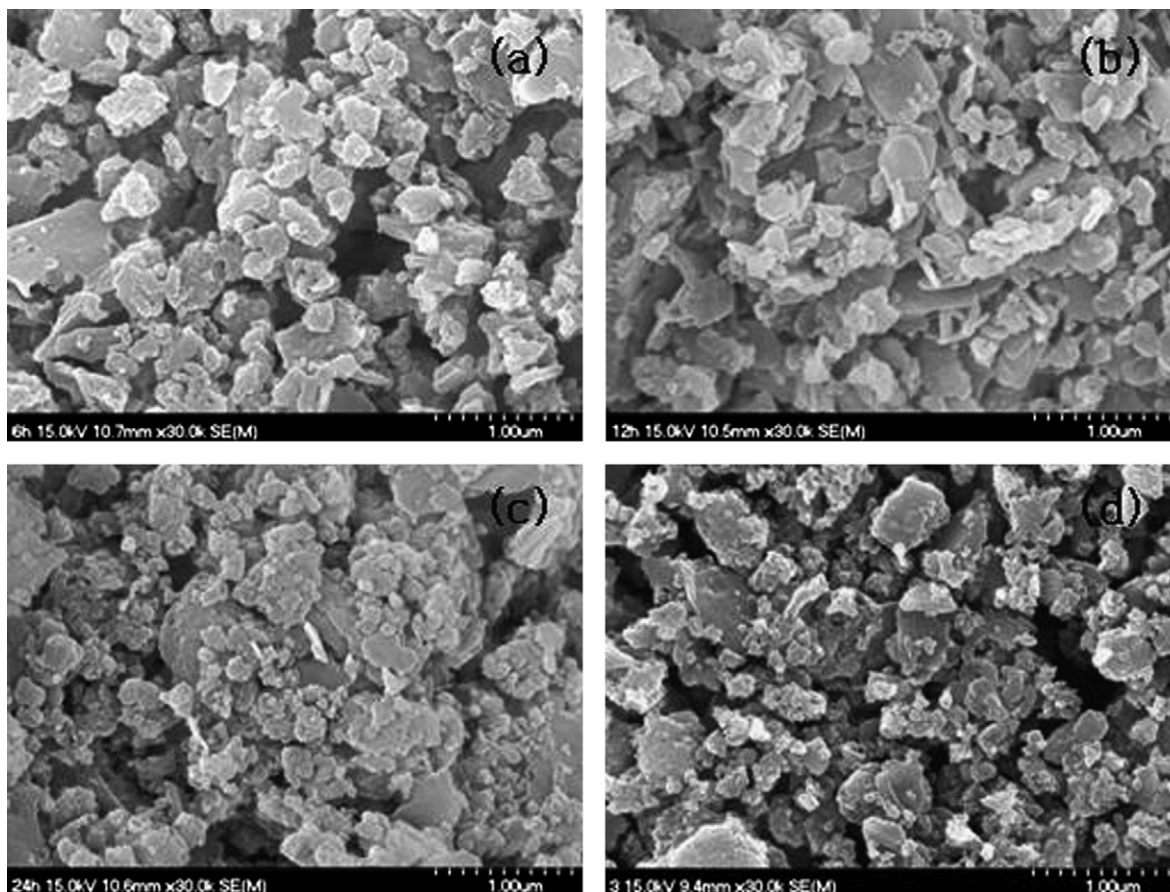
Fig. 8. FE-SEM images of precursor materials prepared by ball-milling for (a) 6 h, (b) 12 h, (c) 24 h and (d) 36 h (heat treatment at 600 °C for 3 h).

In addition, the results revealed that particle size of initial precursor is not associated with generation of the impurity phase Fe_2P. Its discharge capacity is shown in Fig. 9, and the sample
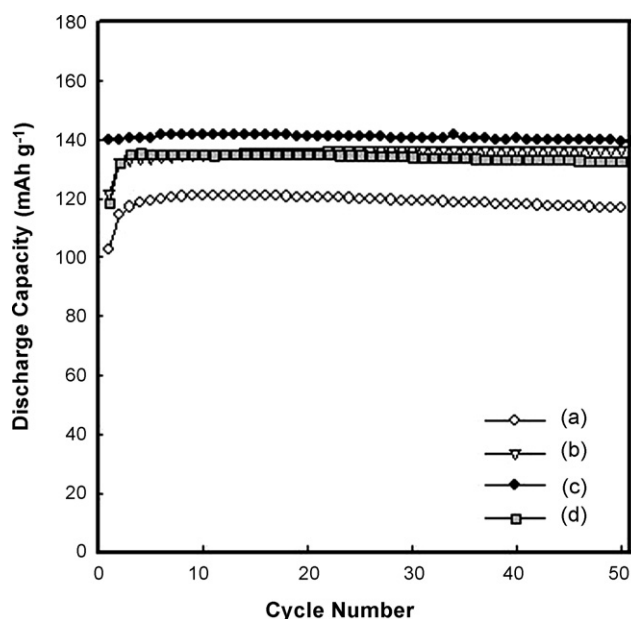

Fig. 9. The discharge capacity of $LiFePO_4$ prepare by ball-milling for (a) 6 h, (b) 12 h, (c) 24 h and (d) 36 h.

ball-milled for 24 h had the best electrochemical performance. The sample ball-milled for 36 h had the smallest crystallite size, and had lower discharge capacity than the sample ball-milled for 24 h. It is likely that the inordinate reduction of crystallite size makes the insertion and extraction of Li^+ ions difficult. On the basis of these results, the optimum processing conditions for obtaining $LiFePO_4$ are ball-milling for 24 h and heat-treatment at 600 °C for 3 h.

The charge and discharge tests at various current rates ranging from 0.1 C to 3 C (1 C = 170 mA g^{-1}) were done to further compare pure $LiFePO_4$ with $LiFePO_4$ containing Fe_2P, and the results are shown in Fig. 10. Pure $LiFePO_4$ was synthesized at 600 °C for 3 h and $LiFePO_4$ with Fe_2P was prepared at 700 °C for 3 h. In the case of the pure $LiFePO_4$/Li cell, the discharge capacity was 160 mAh g^{-1} (93% of theoretical capacity) at 0.1 C; however, it decreased steeply to 90 mAh g^{-1} (56% of its initial value) at the high current rate of 3 C. This is due, in large part, to low diffusion rate of lithium ions for limiting the supply of electrons into the cathode materials [33]. On the contrary, the discharge capacity of $LiFePO_4$ with Fe_2P was 150 mAh g^{-1} at 0.1 C (88% of theoretical capacity) and 104 mAh g^{-1} (69% of its initial value) at 3 C, respectively. This demonstrated that improvement of the electronic conductivity of inter-particles by the effect of Fe_2P can further improve the capacity at high current rate in spite of its large particle size.
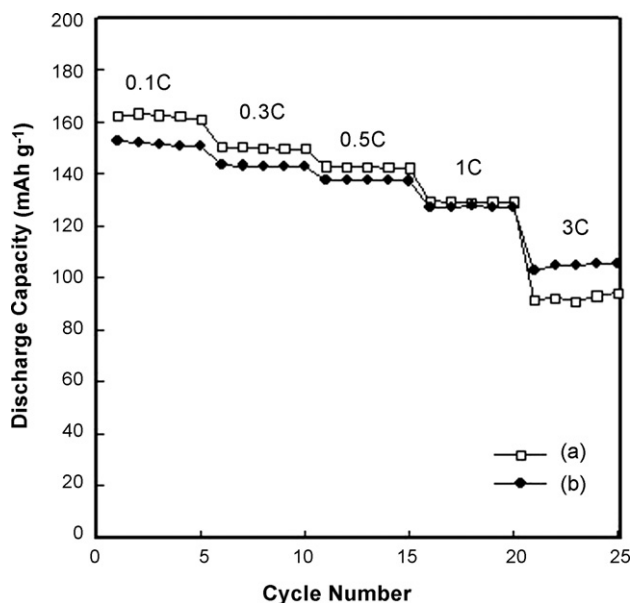
Fig. 10. The rate performance of (a) LiFePO$_4$ prepared at 600 °C for 3 h and (b) LiFePO$_4$ with Fe$_2$P prepared at 700 °C for 3 h. The sample was cycled 5 times at each rate and forwarded to the next step.

4. Conclusions

LiFePO$_4$ has been synthesized successfully by a solid-state reaction method including a one-step heat treatment and ball-milling. The XRD results indicated that the impurity phase Fe$_2$P is detected only in samples prepared at 700 °C. Moreover, this sample had the largest particle size. The effect of impurity phase Fe$_2$P on the electrochemical performance of LiFePO$_4$ was an initial loss and then a gradual increase in discharge capacity upon cycling. The optimum synthesis conditions for obtaining pure LiFePO$_4$ based on the cycling performance were found to be ball-milling for 24 h and heat-treatment at 600 °C for 3 h. This sample had a discharge capacity of 160 mAh g^{-1} at 0.1 C and stable cycle performance. LiFePO$_4$ with Fe$_2$P displayed an excellent high-rate capacity of 104 mAh g^{-1} at 3 C, compared to pure LiFePO$_4$ with a high-rate capacity of 90 mAh g^{-1} at 3 C.

References

[1] M. Winter, J.O. Besenhard, M.E. Spahr, P. Nova'k, Adv. Mater. 10 (1998) 725.
[2] N. Terada, T. Yanagi, S. Arai, M. Yoshikawa, K. Ohta, N. Nakajima, N. Arai, J. Power Sources 100 (2001) 80.
[3] K. Striebel, A. Guerfi, J. Shim, M. Armand, M. Gauthier, K. Zaghib, J. Power Sources 119–121 (2003) 951–954.
[4] K. Mizushima, P.C. Jones, P.C. Wiseman, J.B. Goodenough, Mater. Res. Bull. 15 (1980) 783.
[5] A.K. Padhi, K.S. Najundaswamy, J.B. Goodenough, J. Electrochem. Soc. 144 (1997) 1188.
[6] A.K. Padhi, K.S. Nanjundaswamy, C. Masquelier, S. Okada, J.B. Goode-nough, J. Electrochem. Soc. 144 (1997) 1609.
[7] M.S. Whittingham, Y. Song, S. Lutta, P.Y. Zavalij, N.A. Chernova, J. Mater. Chem. 15 (2005) 3362.
[8] A. Yamada, S.C. Chung, K. Hinokuma, J. Electrochem. Soc. 148 (2001) A224.
[9] A.S. Andersson, J.O. Thomas, B. Kalska, L. Häggström, Electrochem. Solid State Lett. 3 (2000) 66.
[10] D. Morgan, A. Van der Ven, G. Ceder, Electrochem. Solid-State Lett. 7 (2004) A30.
[11] S. Okada, S. Sawa, M. Egashira, J. Yamaki, M. Tabuchi, H. Kageyama, T. Konishi, A. Yoshino, J. Power Sources 97–98 (2001) 430.
[12] H. Huang, S.C. Yin, L.F. Nazar, Electrochem. Solid State Lett. 4 (2001) A170.
[13] J.F. Ni, H.H. Zhou, J.T. Chen, X.X. Zhang, Mater. Lett. 59 (2005) 2361.
[14] D. Wang, H. Li, S. Shi, X. Huang, L. Chen, Electrochim. Acta 50 (2005) 2955.
[15] S.Y. Chung, J.T. Bloking, Y.M. Chiang, Nat. Mater. 1 (2002) 123.
[16] G. Arnold, J. Garche, R. Hemmer, S. Strőbele, C. Vogler, M. Wohlfahrt-Mehrens, J. Power Sources 119-121 (2003) 247.
[17] H.-S. Kim, B.-W. Cho, W. Cho, J. Power Sources 132 (2004) 235.
[18] Y. Hu, M.M. Doeff, R. Kostecki, R. Finones, J. Electrochem. Soc. 151 (2004) A1279.
[19] S.-J. Kwon, C.-W. Kim, W.-T. Jeong, K.-S. Lee, J. Power Sources 137 (2004) 93.
[20] C.-W. Kim, J.-S. Park, K.-S. Lee, J. Power Sources 163 (2006) 144.
[21] J.-K. Kim, G. Cheruvally, J.-W. Choi, J.-U. Kim, J.-H. Ahn, G.-B. Cho, K.-W. Kim, H.-J. Ahn, J. Power Sources 166 (2007) 211.
[22] K.-S. Park, J.-T. Son, H.-T. Chung, S.-J. Kim, C.-H. Lee, H.-G. Kim, Electrochem. Commun. 5 (2003) 839.
[23] R. Janet, D. Guĭerard, Prog. Mater. Sci. 50 (2005) 1.
[24] P. Subramanya Herle, B. Ellis, N. Coombs, L.F. Nazar, Nat. Mater. 3 (2004) 147.
[25] Y.H. Rho, L.F. Nazar, L. Perry, D. Ryan, J. Electrochem. Soc. 154 (2007) A283.
[26] H. Fujii, T. Hokabe, T. Kamigaichi, T. Okamoto, J. Phys. Soc. Jpn. 43 (1977) 41.
[27] P.P. Prosini, M. Carewska, S. Scaccia, P. Wisniewski, S. Passerini, M. Pasquali, J. Electrochem. Soc. 149 (2002) 886.
[28] D.-H. Kim, J.-K. Kim, Electrochem. Solid-State Lett. 9 (2006) A439.
[29] N. Meethong, H-Y.S. Huang, W. Craig Carter, Y.-M. Chiang, Electrochem. Solid-State Lett. 10 (2007) A134.
[30] A.S. Andersson, J.O. Thomas, J. Power Sources 97–98 (2001) 498.
[31] S.S. Zhang, J.L. Allen, K. Xu, T.R. Jow, J. Power Sources 147 (2005) 234–240.
[32] S. Yang, Y. Song, K. Ngala, P.Y. Zavalij, M.S. Whittingham, J. Power Sources 119–121 (2003) 239.
[33] D.-Y.W. Yu, K. Donoue, T. Inoue, M. Fujimoto, S. Fujitani, J. Electrochem. Soc. 153 (2006) A835.